The TAT-JNK inhibitor peptide interferes with beta amyloid protein stability

Cell Death and Differentiation (2007) **14,** 1845–1848; doi:10.1038/sj.cdd.4402202; published online 20 July 2007

Dear Editor,

Alzheimer's disease (AD), the most frequent neurodegenerative disorder in the elderly,[1] is a multifactorial syndrome linked to abnormal metabolism of the transmembrane amyloid precursor protein (APP).[2] Extracellular deposits known as neuritic plaques, a typical neuropathological feature of AD brains, contain large amounts of amyloid-beta-peptide (Aβ), generated from APP by two endoproteolytic cleavages.[3] The biological origin of Aβ plaques and the mechanism whereby Aβ is involved in AD pathogenesis is still elusive and, despite years of research, the normal functions of APP and its catabolites are also not fully understood.

Proteolysis of APP is regulated not only by the secretase enzymes, but also by a cell signal paradigm,[4] although little is known about the intracellular pathways underlying this processing. Disturbance of normal APP processing may contribute to the disease process as well.[5] Again, very little is known about the biological function of the C-terminal intracellular region (AICD) from which the APP domain is cleaved off by γ-secretase.[6]

The importance of this region is now becoming clearer and several studies have examined the signal transduction pathways that interact with this intracellular portion. Thus, independently of secretases, APP is also cleaved by caspase between Asp664 and Ala665 in the AICD intracellular domain.[7,8] The AICD cytosolic domain of APP is the center of a complex network of protein–protein interactions, including c-Jun N-terminal kinase (JNK)-interacting protein-1b (JIP-1b).[9] JIP-1 is a scaffold protein for JNKs and their upstream kinases, MKK7 and MKL3,[10] and may couple APP to the JNK mitogen-activated protein kinase signalling pathway. A recent study using microarray analysis indicated potent APP-dependent expression of c-jun.[11]

We focused on JNK's role in APP phosphorylation in cortical neurons, using the JNK inhibitor D-JNKI1. This cell-permeable, biologically active peptide consists of the JNK-binding domain of JIP-1/IB1 (JBD_{20}), and the HIV-TAT 48–57 transporter sequence[12] and can specifically inhibit JNK in cortical neurons, enabling us to study APP phosphorylation in physiological conditions.

To study the effect of D-JNKI1 on APP processing in primary cultures, adult rat cortical neurons were treated for 24 h with D-JNKI1 at doses of 2, 4 and 6 μM. We used three different antibodies in WB analysis: 22C11, 6E10 and βAPPs. The first recognizes the full length of APP (mature and immature), the βAPPs and αAPPs, the 6E10 antibody identifies only the α cut (the αAPPs), and the βAPPs antibody is specific for β secretase cleavage.

The low concentration, 2 μM D-JNKI1, reduced the APP level (mature form) by 20% in cortical neuron lysates (Figure 1a and b). At 4 μM, APP was reduced by 45% and at 6 μM by 60%. The immature form of APP also declined with 4 and 6 μM, but the decrease was significant only with 6 μM (24%, Figure 1a and b). Thus, D-JNKI1 reduced the levels of both mature and immature APP in neuron lysates.

There was a clear decrease in the secreted APP (APPs) in the media of treated neurons: 2 and 4 μM produced a drop of 30% and 6 μM arrived at a 64% reduction (Figure 1a and b). This confirmed the drop in APP with the peptide on the total lysates. The level of βAPPs dropped significantly in neurons treated with 4 and 6 μM of D-JNKI1, but 2 μM had no significant effect. The βAPPs level fell 30% with 4 μM and 40% with 6 μM (Figure 1a and b).

The same quantification was carried out to distinguish the αAPPs; αAPPs did not decrease with 2 μM, but it dropped 20% with 4 μM and 30% with 6 μM (Figure 1a and b). The αAPPs and βAPPs presented nearly the same reduction. We also analyzed the media of these neurons with the Beta ELISA kit to measure the production of Aβ fragments. There was a dose-dependent reduction: both Aβ1-40 and Aβ1-42 dropped 10% with 2 μM of D-JNKI1, 20% with 4 μM and 30% with 6 μM. This suggests there are no differences between Aβ1-40 and Aβ1-42 fragment production (Figure 1c).

Western blot analysis for P-APP in cortical neuron lysates enabled us to correlate APP phosphorylation and its processing and stability. We used the anti-P-APP-Thr^{668} antibody, which specifically recognizes only this phosphorylated site of the protein, to evaluate D-JNKI1's inhibitory effect. D-JNKI1 prevented phosphorylation at Thr^{668}: 2 μM reduced P-APP by 15% and phosphorylation dropped approximately 55% with 4 and 6 μM (Figure 1a and b). D-JNKI1 powerfully prevented the phosphorylation of APP at Thr^{668} and this strongly correlates with the decline of processing: αAPPs, βAPPs and Aβ fragment production were in fact inhibited.

To further analyze the peptide's effect, we investigated P-APP in cortical neurons by immunofluorescence. Staining was sparse and diffusely distributed in the soma, nuclei and dendrites of control neurons, whereas after 24 h exposure to 4 μM D-JNKI1, P-APP was markedly reduced and localized in the perinuclear and nuclear regions (Figure 1d, upper panels). This confirmed the strong P-APP reduction seen with Western blots and showed relocalization inside neurons due to D-JNKI1's inhibitory effect on APP.

Immunofluorescence for P-c-jun was also used to verify the real inhibitory effect of D-JNKI1. In the control condition,

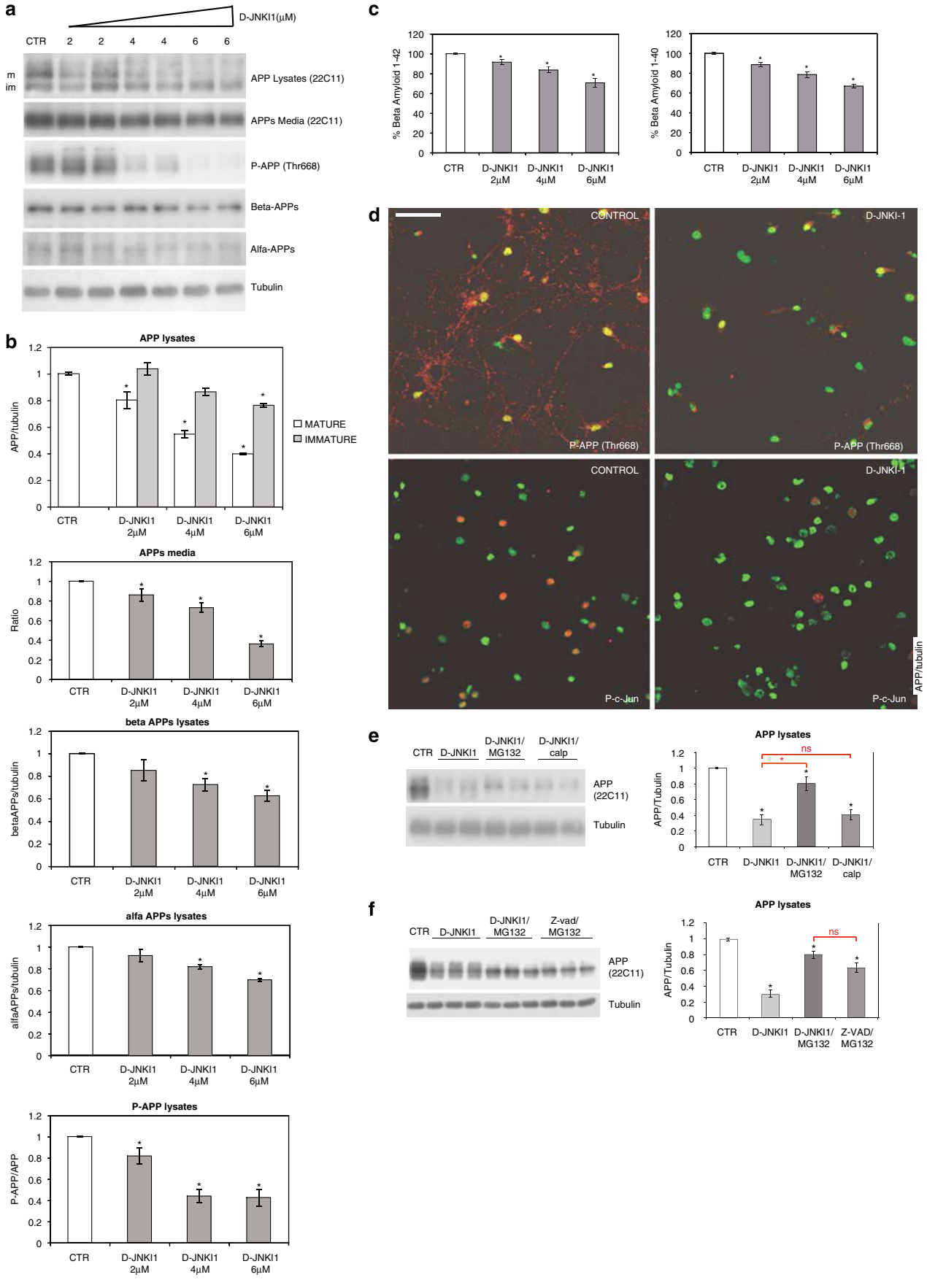
a
D-JNKI1(μM)
CTR 2 2 4 4 6 6
m
im
APP Lysates (22C11)
APPs Media (22C11)
P-APP (Thr668)
Beta-APPs
Alfa-APPs
Tubulin
b
APP lysates
APP/tubulin
MATURE
IMMATURE
APPs media
Ratio
beta APPs lysates
betaAPPs/tubulin
alfa APPs lysates
alfaAPPs/tubulin
P-APP lysates
P-APP/APP
CTR
D-JNKI1 2μM
D-JNKI1 4μM
D-JNKI1 6μM
c
% Beta Amyloid 1-42
% Beta Amyloid 1-40
d
CONTROL
D-JNKI-1
P-APP (Thr668)
P-c-Jun
APP/tubulin
e
CTR
D-JNKI1
D-JNKI1/ MG132
D-JNKI1/ calp
APP (22C11)
Tubulin
APP lysates
APP/Tubulin
ns
f
Z-vad/ MG132

many cortical neurons presented nuclear staining of P-c-jun, because JNK has high basal activity in neurons. After 24 h exposure to the peptide at 4 μM, P-c-Jun labelling was markedly reduced into very few neuronal nuclei (Figure 1d, lower panels).

A recent study proposed a connection between APP expression and the JNK pathway.[11] To clarify D-JNKI1's effect on APP, we investigated whether it affected APP expression besides APP degradation. We compared APP expression in cortical neurons treated for 24 h with 6 μM D-JNKI1 and in untreated neurons, using real-time reverse transcription PCR. APP transcript levels were normalized to the tubulin gene unaltered by the peptide. The results clearly showed that APP expression was not changed by D-JNKI1 (data not shown). D-JNKI1 6 μM for 24 h did not change mRNA expression in rat cortical neurons ($P > 0.05$, four per group), so we concluded that inhibition of JNK/c-Jun pathway did not influence APP expression.

As both mature and immature full-length APP levels in neuron lysates dropped after D-JNKI1 treatment, we investigated whether D-JNKI1 caused APP degradation and whether calpains or the ubiquitin–proteolytic pathways were implicated. Cortical neurons were pre-treated with calpastatin (a specific calpain inhibitor) or with MG132 (a proteasome inhibitor against the 26S complex) and D-JNKI1, resulting in co-treatment of inhibitors. Western blotting showed that APP degradation after D-JNKI1 was strongly inhibited by MG132-D-JNKI1, but not by calpastatin–D-JNKI1 (Figure 1e). Thus, calpains are not involved in APP degradation, and the proteasome pathway is responsible after D-JNKI1 treatment.

Proteasome inhibition had a number of different effects in cells, including caspase 3 activation[13] and APP is a substrate of caspase 3 that cleaves APP in the AICD region.[7] We therefore examined APP levels after co-treatment with MG132 and Z-vad: the effect of Z-vad/MG132 did not differ significantly from D-JNKI1/MG132 (Figure 1f). We conclude that caspase-mediated cleavage of APP is independent of proteasomal activity, whereas APP degradation mediated by D-JNKI1 is proteasome-dependent.

These results indicate that phosphorylation of AICD at Thr^{668} is important for both APP cleavage and degradation in cortical neurons in physiological conditions.

APP is a type I membrane protein of unknown function, whose proteolytic processing, driven by beta- and gamma-secretases, generates the Aβ, one of the pathogenic hallmarks of AD. Its function is unfortunately still poorly understood. Little is known about the AICD/C-terminal cytoplasmic domain that regulates complex protein–protein interactions and intracellular pathways. APP is phosphorylated at multiple sites in the C-terminal cytoplasmic domain[14] and the phosphorylation of Thr^{668} is well established, because it induces conformational changes that affect APP function and metabolism.[15]

Lee *et al.*[16] reported that phosphorylated APP, especially phosphorylated at the Thr^{668}/C-terminal fragment, accumulated to a high level in human AD brain, raising the logical possibility that this phosphorylation may increase Aβ generation. Activated JNK is significantly increased in AD and is localized in the cytoplasm of neurons, the pattern correlating with the progression of the disease.[17] However, the physiological functions of APP phosphorylation at Thr^{668} in neurons remain largely unknown and some possible functions of APP may be clarified by studies of the AICD domain and its partners.

Overall, these results suggest that the cytosolic AICD domain of APP is the center of a complex network that is vital in regulating APP stability. In particular, phosphorylation at Thr^{668} in the AICD appears essential for the regulation of APP stability. Inhibition of JNK-mediated phosphorylation of APP causes it to enter the proteasome pathway, supporting the notion that the phosphorylation state of Thr^{668} is important in its stability and cleavage. The immunofluorescence approach indicates that P-APP is not only reduced by the peptide, but also re-distributed inside neurons. It is normally localized in soma and dendrites and nuclei of cortical neurons,[18] whereas D-JNKI1 treatment limited P-APP staining and distribution to the perinuclear region and nuclei.

We can thus conclude that the D-JNKI1 peptide has an important and selective impact on APP stability: by inhibiting APP phosphorylation at Thr^{668} it helps reduce the production of βAPPs and Aβ fragments and may therefore be important in reducing the neuronal degeneration in AD pathology. These results clearly suggest the AICD domain is an attractive candidate target for new therapeutic approaches.

Acknowledgements. This work was supported by grants from the Botnar Foundation and FNRS (Swiss National Science Foundation) 310000-107888. Dr Repici was supported by a Novartis grant. D-JNKI1 peptide was kindly

Figure 1 (**a**) Effects of JNK inhibition on APP processing in cortical neurons. Cortical neurons were pre-treated with 2, 4 and 6 μM of D-JNKI1 for 24 h and cell lysates were immunoblotted for APP (22C11 antibody), βAPPs, αAPPs and P-APP (Thr^{668}). Loading control, tubulin. There were dose-dependent reductions of APP (m = mature APP and im = immature APP), βAPPs, and αAPPs production and APP phosphorylation. Proteins in the culture media were precipitated and immunoblotted for APPs and the peptide reduced the APPs level. (**b**) Western blot densitometry clearly showed that the peptide reduced APPs, βAPPs, αAPPs and P-APP levels. Quantifications were from eight independent experiments ($\pm$S.E.M.); *$P < 0.05$ *versus* control. (**c**) Quantitative determination of beta-amyloid fragments (1–40 and 1–42) in culture media by ELISA assay. The peptide had the same effect on Aβ 1–40 and Aβ 1–42 (10% decrease with 2 mM D-JNKI1, 20% with 4 mM and 30% with 6 mM). Data are mean of eight independent experiments ($\pm$S.E.M.), *$P \leqslant 0.05$ *versus* control. (**d**) P-APP and P-c-jun immunofluorescence. Left-hand panels show control neurons, right-hand panel neurons treated with 4 μM D-JNKI1 for 24 h, after which the neurons were stained with P-APP (Thr^{668}) antibody, red (upper panels) and P-c-Jun antibody, red (lower panels), and nuclei were counterstained with syto13 reagent, green. In the control condition, P-APP labelling was diffusely distributed in soma, dendrites and nuclei of cortical neurons. D-JNKI1 strongly reduced the labelling, limiting it to the perinuclear and nuclear regions. P-c-jun staining was strongly reduced by D-JNKI1 pre-treatment. Scale bar, 50 μm. (**e**) APP degradation. D-JNKI1 treatment (6 μM) induced APP degradation (65%), whereas co-treatment with MG132 (5 μM) prevented it (reducing APP degradation to 20%). The calpain inhibitor calpastatin had no such effect (2 μM). Quantification was carried out on six independent experiments ($\pm$S.E.M.); *$P < 0.05$ *versus* control. In red, statistical comparison between D-JNKI1 and (1) the co-treatment D-JNKI1/MG132 and (2) D-JNKI1/calpastatin; red asterisk = significant difference determined by Tukey's test. (**f**) APP degradation. Co-treatment with Z-vad (10 μM) and MG132 had minor effect on APP degradation (35%). Red lines indicate the comparison between D-JNKI1/MG132 and z-vad/MG132 by Tukey's test: there is no significant difference. Quantification was carried out on three independent experiments ($\pm$S.E.M.); *$P < 0.05$ *versus* control

provided by Xigen, SA. We thank Catherine Centeno for assistance, Professor P Davis for kindly providing us the specific anti-P-APP antibody, and JD Baggott for revising the manuscript.

A Colombo[1], M Repici[2], M Pesaresi[1], S Santambrogio[1], G Forloni[1] and T Borsello[*,1,2]*

[1] Biol. Neurodeg. Disorders Lab, Istituto di Ricerche Farmacologiche 'Mario Negri', Via Eritrea, Milano, Italy and
[2] Département de Biologie cellulaire et de Morphologie, Université de Lausanne, Switzerland
[*] Corresponding author: T Borsello, Biol. Neurodeg. Disorders Lab, Istituto di ricerche Farmacologiche, 'Mario Negri', Via Eritrea 62, Milano 20157, Italy. Tel: +39 02 39 014 469; Fax: +39 02 354 6277; E-mail: borsello@marionegri.it and Département de Biologie Cellulaire et de Morphologie, Université de Lausanne, CH-1005, Switzerland. Tel: +41 21 692 5277; Fax: +41 21 692 5105; E-mail: Tiziana.Borsello@unil.ch

1. Hedera P, Turner RS. *Neurol Clin* 2002; **20**: 779–808, vii.
2. Selkoe DJ. *Physiol Rev* 2001; **81**: 741–766.
3. Kalback W, Watson MD, Kokjohn TA, Kuo YM, Weiss N, Luehrs DC *et al. Biochemistry* 2002; **41**: 922–928.
4. Brown MS, Ye J, Rawson RB, Goldstein JL. *Cell* 2000; **100**: 391–398.
5. Stokin GB, Lillo C, Falzone TL, Brusch RG, Rockenstein E, Mount SL *et al. Science* 2005; **307**: 1282–1288.
6. LaFerla FM. *Nat Rev Neurosci* 2002; **3**: 862–872.
7. Takeda K, Araki W, Akiyama H, Tabira T. *Faseb J* 2004; **18**: 1755–1757.
8. Taru H, Yoshikawa K, Suzuki T. *FEBS Lett* 2004; **567**: 248–252.
9. Taru H, Kirino Y, Suzuki T. *J Biol Chem* 2002; **277**: 27567–27574.
10. Whitmarsh AJ, Kuan CY, Kennedy NJ, Kelkar N, Haydar TF, Mordes JP *et al. Genes Dev* 2001; **15**: 2421–2432.
11. Kogel D, Schomburg R, Copanaki E, Prehn JH. *Cell Death Differ* 2005; **12**: 1–9.
12. Bonny C, Oberson A, Negri S, Sauser C, Schorderet DF. *Diabetes* 2001; **50**: 77–82.
13. Flood F, Murphy S, Cowburn RF, Lannfelt L, Walker B, Johnston JA. *Biochem J* 2005; **385** (Part 2): 545–550.
14. Suzuki T, Oishi M, Marshak DR, Czernik AJ, Nairn AC, Greengard P. *EMBO J* 1994; **13**: 1114–1122.
15. Ramelot TA, Nicholson LK. *J Mol Biol* 2001; **307**: 871–884.
16. Lee MS, Kao SC, Lemere CA, Xia W, Tseng HC, Zhou Y *et al. J Cell Biol* 2003; **163**: 83–95.
17. Zhu X, Raina AK, Rottkamp CA, Aliev G, Perry G, Boux H *et al. J Neurochem* 2001; **76**: 435–441.
18. Muresan Z, Muresan V. *C J Cell Biol* 2005; **171**: 615–625.

Calreticulin exposure is required for the immunogenicity of γ-irradiation and UVC light-induced apoptosis

Cell Death and Differentiation (2007) **14,** 1848–1850; doi:10.1038/sj.cdd.4402201; published online 27 July 2007

Dear Editor,

It is commonly assumed that the only goal of anticancer chemotherapy, like antimicrobial antibiotic therapy, is to eradicate by direct cytotoxic effects all tumor cells. According to this mechanism, complete and permanent cure would be obtained by antineoplastic agents that succeed in killing all cancer cells including cancer stem cells and micrometastases.[1,2] In fact, cancer has long been conceived and treated as a cell-autonomous phenomenon, regardless of the immune system's contribution to the therapeutic response. Recently, we have challenged this idea by showing that, at least in the case of anthracyclin-mediated chemotherapy, the antitumor immune response plays a major role in therapeutic success. Thus, immunocompetent mice bearing CT26 colon carcinomas or MCA205 fibrosarcomas can be cured by intratumoral injection of anthracyclins, whereas immunodeficient mice lacking T cells only exhibit partial responses with a delay in tumor growth.[3–5] Detailed molecular studies revealed that anthracyclins have the peculiar capacity of inducing immunogenic cell death. In contrast, many other cytotoxic agents including agents that damage nuclear DNA (such as etoposide and mitomycin C), mitochondria, the endoplasmic reticulum or lysosomes fail to induce immunogenic cell

Figure 1 Early CRT exposure is required for the immunogenic effect of γ-irradiation or UVC light exposure. (**a**, **b**) Kinetics of PS exposure and cell death induced by γ-irradiation (**a**) or UVC light (**b**). CT26 colon cancer cells cultured in RPMI 1640 medium supplemented with 10% FCS, penicillin, streptomycin, 1 mM pyruvate and 10 mM HEPES and treated by γ-irradiation (75 Gy) or UVC light (100 J/cm^2). After the indicated time period, cells were trypsinized and stained with FITC-labelled annexin V and propidium iodide following standard protocols,[21] and subjected to cytofluorometric analyses. Numbers in each quadrant refer to the percentage of cells (X$\pm$S.E.M. of triplicates). (**c**, **d**) Immunofluorescence detection of CRT exposure on the cell surface in response to γ-irradiation (**c**) or UVC light (**d**). Cells treated as above were stained for the detection of surface CRT as described[4] 1 h after treatment. Representative cells are shown. (**e**, **f**) Kinetics of CRT exposure determined by FACS analysis after γ-irradiation (**e**) or UVC light (**f**). Cells treated as in panels **a** and **b** were trypsinized and stained for the detection of CRT on the cell surface while gating on the viable population and excluding dead cells staining with propidium iodide. The CRT-specific staining profiles, as obtained for each time point post-treatment, are compared with those of untreated cells. (**g**, **h**) Manipulation of CRT exposure by an siRNA and adsorption of recombinant CRT protein. Cells were transfected with a control siRNA or a CRT-specific siRNA heteroduplex (sense strand: 5′-rCrCrGrCUrGrGrGUrCrGrArAUrCrRrArATT-3′). Thirty-six hours later, the cells were subjected to γ-irradiation (**g**) or UVC light (**h**), cultured for 4 h, optionally treated with recombinant CRT protein (3 μg/10^6 cells in PBS on ice for 30 min, followed by three washes) and subjected to immunofluorescence staining of CRT as above. (**i**, **j**) Requirement of CRT exposure for the immunogenic effect of ionizing irradiation. CT26 colon cancer cells were transfected with the indicated siRNAs, γ-irradiation (**i**), UV light (**j**) and/or recombinant CRT (as in **g** and **h**) and then injected subcutaneously (3 $\times$ 10^6 cells) into the left flank of BALB/c mice. One week after this vaccination, the mice were challenged with live tumor cells in the opposite flank (day 0) and the frequency of tumor-free animals was monitored (mean$\pm$S.E.M.); *n* represents the absolute number of mice enrolled in each cohort. *$P<0.001$ (Student's *t*-test)